Short Article

Cell Stem Cell

The Long Noncoding RNA *Pnky* Regulates Neuronal Differentiation of Embryonic and Postnatal Neural Stem Cells

Graphical Abstract

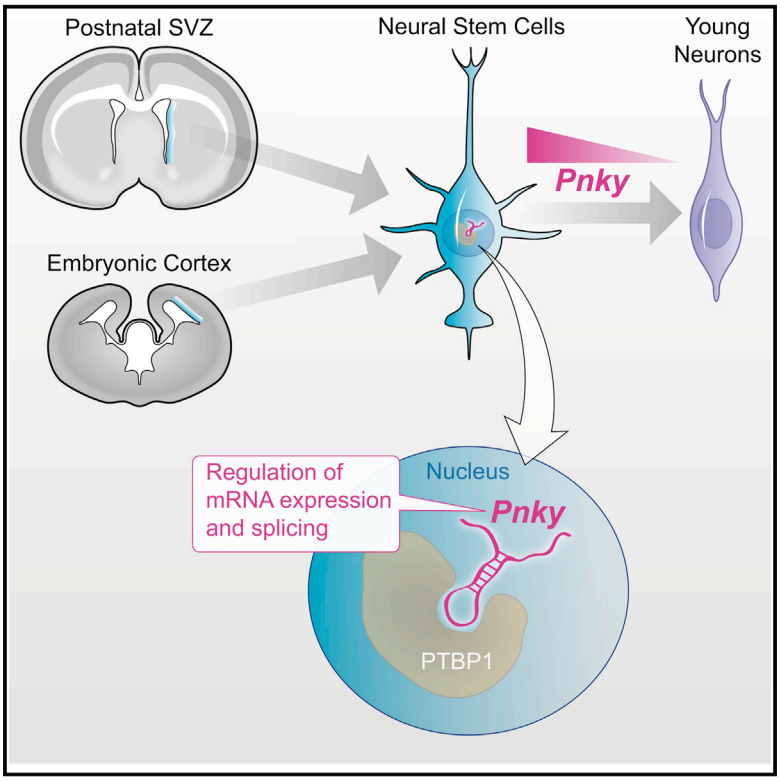

Authors

Alexander D. Ramos, Rebecca E. Andersen, ..., Arnold R. Kriegstein, Daniel A. Lim

Correspondence

daniel.lim@ucsf.edu

In Brief

Ramos et al. describe *Pinky* (*Pnky*), a neural-specific lncRNA that localizes to the nucleus of neural stem cells (NSCs). *Pnky* knockdown in NSCs increases neurogenesis. *Pnky* interacts with splicing regulator PTBP1, and PTBP1 and *Pnky* regulate the expression and splicing of a core set of transcripts related to neuronal differentiation.

Highlights

- The lncRNA *Pnky* is expressed in mouse and human neural stem cells in vivo
- *Pnky* knockdown increases neuronal differentiation in culture and in vivo
- *Pnky* localizes to the nucleus and interacts with the mRNA splicing regulator PTBP1
- PTBP1 and *Pnky* regulate expression of key transcripts related to differentiation

Accession Numbers

GSE65542
KP881340
KP881341

Ramos et al., 2015, Cell Stem Cell *16*, 439–447
April 2, 2015
http://dx.doi.org/10.1016/j.stem.2015.02.007

CellPress

Cell Stem Cell
Short Article

The Long Noncoding RNA *Pnky* Regulates Neuronal Differentiation of Embryonic and Postnatal Neural Stem Cells

Alexander D. Ramos,[1,2,3,9] Rebecca E. Andersen,[1,2,4,9] Siyuan John Liu,[1,2,3] Tomasz Jan Nowakowski,[2,5] Sung Jun Hong,[1,2,7] Caitlyn C. Gertz,[2,5,6] Ryan D. Salinas,[1,2] Hosniya Zarabi,[1,2] Arnold R. Kriegstein,[2,5] and Daniel A. Lim[1,2,8,*]

[1]Department of Neurological Surgery
[2]Eli and Edythe Broad Center of Regeneration Medicine and Stem Cell Research
[3]Medical Scientist Training Program, Biomedical Sciences Graduate Program
[4]Developmental and Stem Cell Biology Graduate Program
[5]Department of Neurology
[6]Neuroscience Graduate Program
University of California, San Francisco, San Francisco, CA 94143, USA
[7]CIRM-Bridges Scholar Program, San Francisco State University, San Francisco, CA 94132, USA
[8]San Francisco Veterans Affairs Medical Center, San Francisco, CA 94121, USA
[9]Co-first author
*Correspondence: daniel.lim@ucsf.edu
http://dx.doi.org/10.1016/j.stem.2015.02.007

SUMMARY

While thousands of long noncoding RNAs (lncRNAs) have been identified, few lncRNAs that control neural stem cell (NSC) behavior are known. Here, we identify *Pinky* (*Pnky*) as a neural-specific lncRNA that regulates neurogenesis from NSCs in the embryonic and postnatal brain. In postnatal NSCs, *Pnky* knockdown potentiates neuronal lineage commitment and expands the transit-amplifying cell population, increasing neuron production several-fold. *Pnky* is evolutionarily conserved and expressed in NSCs of the developing human brain. In the embryonic mouse cortex, *Pnky* knockdown increases neuronal differentiation and depletes the NSC population. *Pnky* interacts with the splicing regulator PTBP1, and PTBP1 knockdown also enhances neurogenesis. In NSCs, *Pnky* and PTBP1 regulate the expression and alternative splicing of a core set of transcripts that relates to the cellular phenotype. These data thus unveil *Pnky* as a conserved lncRNA that interacts with a key RNA processing factor and regulates neurogenesis from embryonic and postnatal NSC populations.

INTRODUCTION

Neural stem cells (NSCs) exist in both the embryonic and postnatal mammalian brain. In the embryonic cortical ventricular zone (VZ) and adult ventricular-subventricular zone (V-SVZ), NSCs are glial cells that can both self-renew and differentiate to yield intermediate progenitors that divide once or more before producing migratory young neurons (Kriegstein and Alvarez-Buylla, 2009). The production of proper numbers of neuronal progenitors from NSCs is a key aspect of brain development, and defects at this stage of the neurogenic lineage may underlie a number of human developmental disorders (Lui et al., 2011).

The mammalian genome encodes many thousands of lncRNAs—transcripts over 200 nucleotides (nt) long that have no evidence of protein coding potential—and emerging data indicate that lncRNAs can have critical biological functions (Batista and Chang, 2013; Lee, 2012; Mercer and Mattick, 2013; Rinn and Chang, 2012). Although transcription factors, microRNAs, and signaling pathways that control the transition between NSCs and neurogenic progenitors have been studied intensively (Ihrie and Alvarez-Buylla, 2011; Kriegstein and Alvarez-Buylla, 2009; Lui et al., 2011), lncRNAs that regulate this critical, early stage of neurogenesis have not been identified.

Here we describe the unique developmental function of a neural-specific lncRNA we have named *Pinky* (*Pnky*) and provide insights into its molecular function. We have previously shown that knockdown of lncRNAs *Dlx1as* and *Six3os* in V-SVZ NSCs results in decreased neurogenesis (Ramos et al., 2013). Similarly, loss-of-function studies of different lncRNAs in ESC-derived NSCs (Lin et al., 2014; Ng et al., 2013), zebrafish brain (Ulitsky et al., 2011), and mouse CNS (Bond et al., 2009; Rapicavoli et al., 2011; Sauvageau et al., 2013) all demonstrate a loss of neuronal populations. In contrast, postnatal V-SVZ NSCs with *Pnky* knockdown (*Pnky*-KD) generated 3- to 4-fold more neurons. To understand this phenotype, we used time-lapse microscopy to study lineage commitment and cell proliferation at the single-cell level. We cloned the human *PNKY* transcript and discovered its expression in the VZ of the embryonic human brain, and we demonstrated a role for *Pnky* in the development of the embryonic mouse cortex in vivo. Using mass spectrometry, we found that *Pnky* bound to polypyrimidine tract-binding protein 1 (PTBP1), an RNA-splicing factor that is a

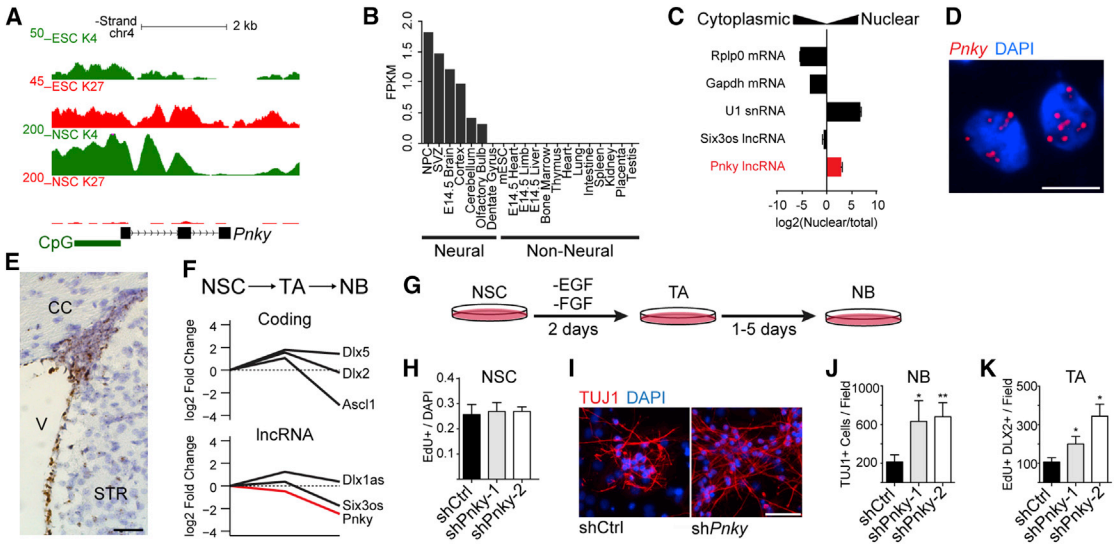

Figure 1. The lncRNA *Pinky* Is Expressed in V-SVZ NSCs and Regulates Neuronal Differentiation

(A) UCSC genome browser view of the *Pnky* locus. Also shown are ChIP-seq tracks for H3K4me3 and H3K27me3 in ESCs and V-SVZ NSCs.

(B) Fragments per kilobase per million mapped reads (FPKM) values for *Pnky* in indicated tissues.

(C) Subcellular fractionation followed by RT-qPCR for indicated lncRNAs and mRNAs. Error bars are propagated SD from technical triplicate wells.

(D) Branched-DNA ISH for *Pnky* in V-SVZ NSC cultures. Nuclei are counterstained with DAPI. Scale bar, 10 μm.

(E) Branched-DNA ISH for *Pnky* (brown) in adult mouse coronal brain section. Nuclei are counterstained with hematoxylin. V, ventricle; CC, corpus collosum; STR, striatum. Scale bar, 50 μm.

(F) Microarray expression analysis from FACS-isolated neural stem cells (NSC), transit-amplifying cells (TA), and neuroblasts (NB). Value in NSCs set to 0.

(G) Schematic of V-SVZ NSC culture system.

(H) Quantification of EdU labeling counted from GFP+ cultures of V-SVZ NSCs infected with control or *Pnky*-KD constructs.

(I) ICC for TUJ1 (red) after 7 days of differentiation in control or *Pnky*-KD GFP+ cultures. Nuclei are counterstained with DAPI (blue). Scale bar, 50 μm.

(J) Quantification of TUJ1+ NBs produced after 7 days of differentiation.

(K) Quantification of the number of TA cells after 2 days of differentiation.

Error bars for (H), (J), and (K) are SD from triplicate wells; *$p < 0.05$, **$p < 0.01$, Student's t test. See also Figure S1.

potent regulator of neural development (Keppetipola et al., 2012), direct cell reprogramming (Xue et al., 2013), and brain tumor growth (Ferrarese et al., 2014). Further analysis indicated that *Pnky* and PTBP1 modulate the expression and alternative splicing of an overlapping set of transcripts, and double knockdown epistasis experiments suggested that *Pnky* and PTBP1 function in the same pathway. Overall, our work demonstrates that an evolutionarily conserved lncRNA can regulate neurogenesis from NSCs in both the embryonic and postnatal brain.

RESULTS

Throughout adult life, V-SVZ NSCs give rise to transit-amplifying (TA) cells, which generate neuroblasts (NBs) that migrate to the olfactory bulb where they differentiate into interneurons (Doetsch et al., 1999; Lois and Alvarez-Buylla, 1994; Luskin, 1998; Peretto et al., 1997). *Pnky* (previously called *lnc-pou3f2*) is an lncRNA that we initially identified as being expressed in the adult V-SVZ (Ramos et al., 2013). RACE (rapid amplification of cDNA ends) cloning followed by Sanger sequencing demonstrated *Pnky* to be an 825 nt polyadenylated RNA encoded from three exons (Figure 1A). Analysis with the Coding Potential Calculator (CPC) (Kong et al., 2007), PhyloCSF (Lin et al., 2011), and the Coding-Potential Assessment Tool (CPAT) (Wang et al., 2013) indicated that the *Pnky* transcript has no protein-coding potential (Figure S1A). Analysis of available RNA-seq datasets indicated that *Pnky* is specifically expressed in neural tissues and lineages but is not expressed in the dentate gyrus, which contains another population of adult NSCs (Figure 1B). Furthermore, like many key developmental genes, the promoter of *Pnky* was "bivalent" with both histone 3 lysine 27-trimethylation (H3K27me3) and histone 3 lysine 4-trimethylation (H3K4me3) in embryonic stem cells (ESCs), coherent with its repressed but "poised" transcriptional state (Figure 1A). In contrast, in ESC-derived NSCs (ESC-NSCs) and V-SVZ NSCs, the *Pnky* promoter was monovalent with H3K4me3, consistent with its active transcription (Figures 1A and S1B).

Nuclear fractionation of V-SVZ NSC cultures followed by RT-qPCR analysis demonstrated *Pnky* to be enriched in the nucleus as compared to coding mRNAs, which were enriched in cell lysates containing cytoplasm (Figure 1C). Consistent with the nuclear fractionation studies, in situ hybridization (ISH) for *Pnky* demonstrated predominantly nuclear localization of the transcript (Figures 1D and S1C).

ISH of adult mouse brain tissue revealed prominent expression of *Pnky* in the V-SVZ (Figure 1E). To investigate whether *Pnky* expression is dynamic within the neurogenic lineage, we analyzed gene expression of V-SVZ cells acutely isolated from the brain through fluorescence-activated cell sorting (FACS) (Ramos et al., 2013). Briefly, activated NSCs express both glial fibrillary acidic protein (GFAP) and the epidermal growth factor receptor (EGFR). TA cells are GFAP− but retain EGFR

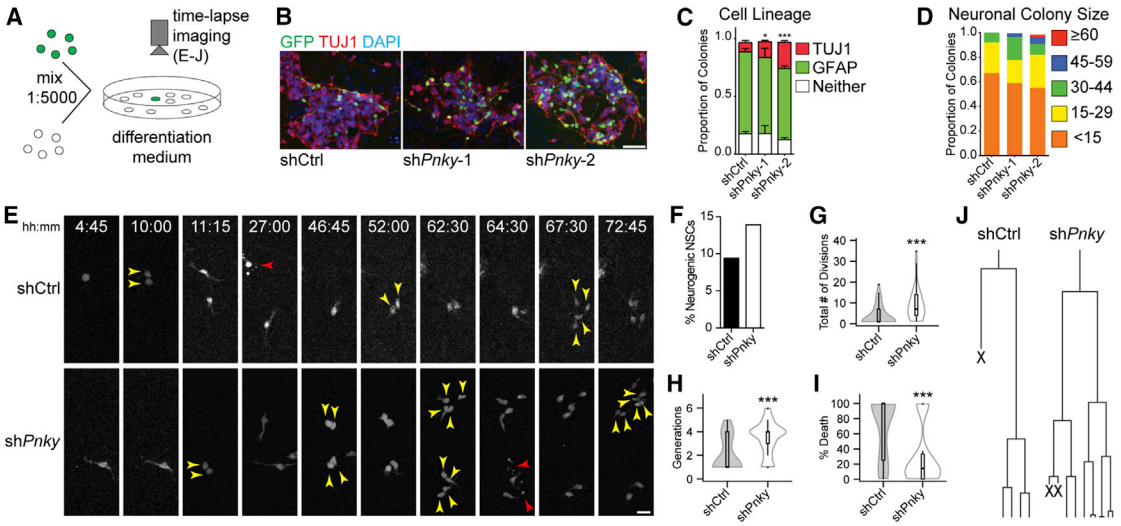

Figure 2. *Pinky* Knockdown Leads to an Expansion of Neurogenic TA Progenitors

(A) Schematic of experimental design.

(B) Representative images of isolated colonies after 4 days of differentiation. Immunocytochemistry (ICC) for TUJ1 (red) and GFP (green). Nuclei are DAPI counterstained (blue). Scale bar, 50 μm.

(C) Quantification of the fate of isolated GFP+ colonies. Error bars = SD of triplicate experiments.

(D) Quantification of TUJ1+ NBs found in individual neurogenic colonies.

(E) Representative frames from time-lapse video of control (top) or *Pnky*-KD (bottom) single cells. Time of differentiation is indicated. Yellow arrows indicate daughter cells resulting from a recent division, and red arrows indicate cell death. Scale bar, 25 μm.

(F) Bar graph representing the percentage of initial tracked progenitors that gave rise to NBs. n = 531 GFP+ shCtrl NSCs and 316 GFP+ sh*Pnky* NSCs.

(G) Violin plots overlaying box-and-whisker plots of total number of divisions undergone by a single initial neurogenic progenitor and all of its daughter cells. n = 44 shCtrl and 33 sh*Pnky* progenitors.

(H) Violin plots overlaying box-and-whisker plots of the number of generations per initial neurogenic progenitor for shCtrl and sh*Pnky*. n = 44 shCtrl and 33 sh*Pnky* progenitors.

(I) Violin plots overlaying box-and-whisker plots of the percentage of progeny per single neurogenic progenitor that underwent cell death. n = 44 shCtrl and 33 sh*Pnky* progenitors.

(J) Tree diagram for the frames shown in (E) and corresponding time-lapse movies. X indicates cell death.

*p < 0.05, ***p < 0.001, Student's t test. See also Figure S2.

expression, and NBs express cell surface marker CD24 (Pastrana et al., 2009). *Pnky* expression was highest in NSCs and decreased by 5.6-fold (p = 0.0003, Student's t test) in migratory NBs (Figure 1F). Thus, *Pnky* is normally downregulated during lineage progression in vivo.

To investigate the role of *Pnky* in neurogenesis, we first used V-SVZ NSC monolayer cultures that recapitulate key features of neuronal differentiation as well as glial cell production (Figure 1G). *Pnky* was expressed in cultured NSCs in self-renewal conditions. Upon differentiation, *Pnky* remained expressed in GFAP+ astrocytes but was downregulated in TUJ1+ neuronal cells (Figure S1D), similar to the pattern of expression seen in vivo. After lentiviral transduction with control (shCtrl-GFP) or *Pnky* (sh*Pnky*-1-GFP and sh*Pnky*-2-GFP) knockdown constructs, GFP+ NSCs were isolated through FACS and cultured. *Pnky* knockdown was efficient in both self-renewing NSCs and after their differentiation (Figures S1E and S1F). Cells in these purified cultures uniformly expressed SOX2, a neural stem cell marker (Figure S1G). Flow cytometric analysis of these infected cells indicated that the majority (66.0%) were also positive for both GFAP and NESTIN (Figure S1H), markers of V-SVZ NSCs. Therefore, the majority of cells transduced with *Pnky*-KD or control vectors were GFAP+, NESTIN+, SOX2+ V-SVZ NSCs.

Pnky-KD NSCs incorporated the thymidine analog 5-ethynyl-2′-deoxyuridine (EdU) at the same rate as control NSCs, suggesting that proliferation in self-renewal conditions was not affected (Figures 1H and S1I). However, *Pnky*-KD NSCs generated 3-fold more TUJ1+ NBs after 7 days of differentiation (Figures 1I and 1J). To further analyze the effect of *Pnky*-KD in the NSC population, we used a molecular-genetic method of targeting knockdown to V-SVZ NSCs (Doetsch et al., 1999; Park et al., 2014). We derived NSC cultures from G-TVA mice, which express the chicken retroviral receptor TVA from the GFAP promoter. For viral transduction of these cultures, we used shRNA lentiviruses pseudotyped with chicken viral EnvA protein, which restricts infection to the GFAP+ cells (Figure S1J). In G-TVA NSCs, *Pnky*-KD did not affect NSC proliferation in self-renewal conditions (Figure S1K). However, after differentiation, G-TVA NSC cultures produced 3.56-fold more NBs as compared to control (Figure S1L). Thus, *Pnky*-KD targeted to the GFAP+ NSC population in V-SVZ cultures also resulted in increased neuronal production during differentiation.

V-SVZ TA cells express DLX2 and normally divide several times before giving rise to NBs (Doetsch et al., 2002; Ponti et al., 2013). With *Pnky*-KD, there were 1.8- to 3.2-fold more EdU+, DLX2+ cells at 2 days of differentiation, suggesting that

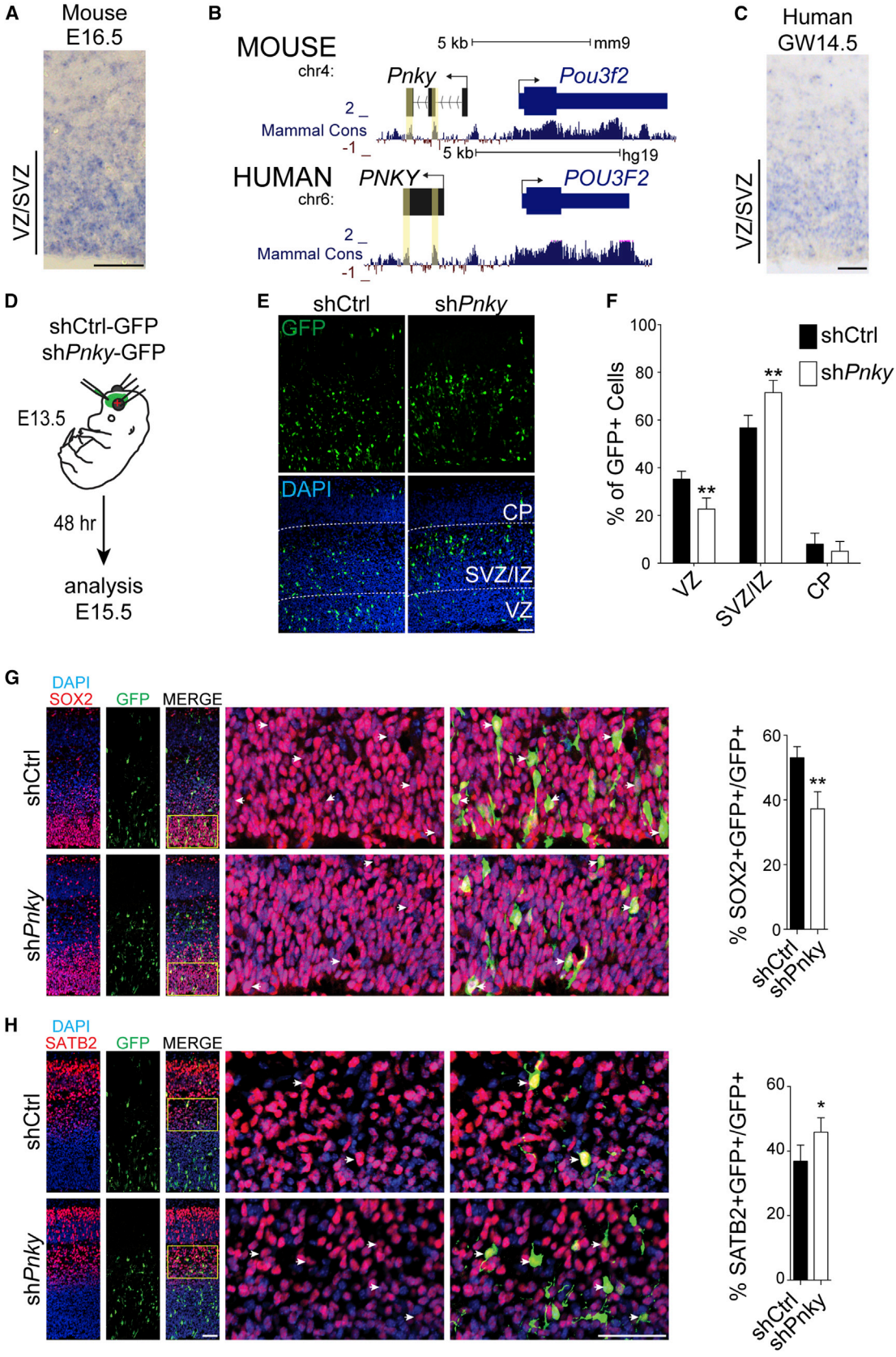

(legend on next page)

Pnky plays a role at the TA stage of neuronal differentiation (Figures 1K and S1M).

To further investigate how *Pnky*-KD increases neuronal production, we plated NSCs infected with *Pnky*-KD or control vector with large numbers of uninfected NSCs (ratio of infected GFP+ NSCs to uninfected NSCs was approximately 1:5,000; Figure 2A). After 4 days of differentiation, these cultures produced well-isolated clusters of GFP+ cells (Figure 2B). With *Pnky*-KD, the proportion of GFP+ cell clusters containing TUJ1+, GFP+ cells was increased (Figure 2C). Furthermore, these clusters also contained greater numbers of TUJ1+, GFP+ NBs (Figure 2D). These data suggested that the increased neurogenesis resulted from both a shift toward neuronal lineage commitment and an increase in cell amplification within the neurogenic lineage.

To more directly observe the clonal behavior of individual NSCs with *Pnky*-KD, we used time-lapse microscopy to image GFP+ cells every 15 min for 3 days (Figure 2E). We followed the fate of 316 GFP+ *Pnky*-KD NSCs and 531 GFP+ control NSCs. After differentiation, we could identify both TUJ1+ neurogenic clones (Figure S2A) and GFAP+ glial clones (Figures S2B and S2C). Clones arising from NSCs with *Pnky*-KD were 48% more likely to be neurogenic (Figure 2F). Thus, *Pnky*-KD increased the likelihood that NSCs produced neurogenic progenitors.

Neurogenic clones with *Pnky*-KD contained 2.74-fold more NBs than control (Figure S2D). This increase in neurogenesis was in part related to an increase in progenitor cell divisions before differentiation into NBs: while control progenitors divided 3.93 (SD = 4.68, n = 44) times and gave rise to 2.05 (SD = 1.42) generations of daughter cells, *Pnky*-KD resulted in 8.94 (SD = 7.64, n = 33) divisions and 3.45 (SD = 1.41) generations (Figures 2G and 2H). The average cell-cycle length was not affected by *Pnky*-KD (19.4 hr versus 19.1 hr, p = 0.89) (Figure S2E), suggesting that the increased number of divisions related to the maintenance of a proliferative cell state and not an accelerated cell cycle. Time-lapse imaging also enabled direct observation of cell death, and the number of GFP+ neurogenic progeny (NBs) that underwent cell death was reduced 57% by *Pnky*-KD (Figure 2I). Thus, *Pnky*-KD promoted neuronal lineage commitment from postnatal V-SVZ NSCs, increased the number of divisions of neurogenic progenitors, and reduced cell death (Figures 2J and S2F).

To investigate whether *Pnky* also regulates neurogenesis from other NSC populations, we next examined the embryonic brain. *Pnky* transcripts were detected in embryonic mouse brain tissue by RNA-seq (Figure 1B), and ISH revealed its expression in the cortical VZ—where embryonic NSCs reside—at embryonic day 14.5 (E14.5) and E16.5 (Figures 3A, S3A, and S3B). *Pnky* has two regions of high conservation among vertebrates (Figures 3B and S3C), and using strand-specific RNA-seq of gestational week 16 (GW16) human cortical samples, we detected a noncoding transcript divergent to *POU3F2* that included the conserved sequences. RACE cloning identified human *PINKY* (*PNKY*) as a polyadenylated 1,592 nt transcript containing the two conserved elements and expressed from a conserved promoter region (Figure 3B). As in the developing mouse brain, ISH of GW14.5 human cortex demonstrated *PNKY* expression in the VZ, with decreased levels in the subventricular zone and intermediate zone (SVZ/IZ), where young neurons begin to differentiate (Figures 3C and S3D).

To investigate the role of *Pnky* in the mouse embryonic VZ, we electroporated *Pnky*-KD (sh*Pnky*-2-GFP) or control (shCtrl-GFP) construct into VZ cells at E13.5 (Figure 3D). Two days later, we analyzed GFP+ cells in the VZ, SVZ/IZ, and cortical plate (CP) (Figure 3E). With *Pnky*-KD, there was a 35% decrease in the proportion of GFP+ cells in the VZ and a 26% increase in GFP+ cells in the SVZ/IZ (Figure 3F). We did not detect apoptotic GFP+ cells as assessed by cleaved caspase-3 staining (not shown). At this time point in cortical development, SOX2+ NSCs in the VZ produce proliferative TBR2+ progenitor cells in the SVZ/IZ that differentiate into SATB2+ young neurons. With *Pnky*-KD, the proportion of SOX2+, GFP+ cells was reduced (Figure 3G). While *Pnky*-KD did not affect the proportion of TBR2+, GFP+ TA cells or their proliferation (Figures S3E–S3J), the proportion of SATB2+, GFP+ young neurons was increased (Figure 3H). These data indicate that *Pnky* regulates the production of young neurons from embryonic brain NSCs in vivo (Figure S3K).

Many lncRNAs regulate gene expression through interactions with specific protein partners. To identify *Pnky*-interacting proteins, we incubated biotinylated *Pnky* (S) or antisense *Pnky* (AS) control RNA with V-SVZ NSC nuclear extract and used mass spectrometry to identify proteins that bound to the transcripts (Figures S4A and S4B). PTBP1 was identified as a binding partner of *Pnky*, and this interaction was confirmed by western blot analysis (Figure 4A). While both *Pnky* and control RNA

Figure 3. *Pinky* Is Expressed in the Developing Mouse and Human Cortex and Regulates the Differentiation of Mouse Cortical Progenitors In Vivo

(A) ISH for *Pnky* in embryonic day 16.5 (E16.5) mouse brain.

(B) Genome browser track showing two regions of high conservation, determined by PhyloP score (yellow boxes). Human *PNKY* genomic region is shown below with conservation indicated. For clarity, the mouse strand is shown left to right.

(C) ISH for *PNKY* in gestational week 14.5 (GW14.5) human brain.

(D) Schematic of in utero electroporation of mouse embryonic brain.

(E) Cortical sections at E15.5, 2 days after electroporation with shCtrl (left) or sh*Pnky* (right). Immunohistochemistry (IHC) for GFP (top) and with DAPI counterstain (bottom) is shown. VZ, ventricular zone; SVZ/IZ, subventricular zone/intermediate zone; CP, cortical plate.

(F) Quantification of GFP+ cell distribution in indicated zones as a percentage of total GFP+ cells.

(G) Left: cortical sections at E15.5, 2 days after electroporation with shCtrl or sh*Pnky*. IHC for GFP (green) and SOX2 (red), with DAPI nuclear counterstain (blue), is shown. Yellow box indicates region enlarged in the adjacent panels. Arrowheads indicate co-labeled cells. Right: quantification of SOX2+, GFP+ cells as a percentage of total GFP+ cells.

(H) Left: Cortical sections immunostained for GFP (green) and SATB2 (red), with DAPI nuclear counterstain (blue). Yellow box indicates region enlarged in the adjacent panels. Right: quantification of SATB2+, GFP+ cells as a percentage of total GFP+ cells.

All error bars are S.D., n = 4 brains of each condition from three separate surgeries. *p < 0.05, **p < 0.01. All scale bars, 50 μm. See also Figure S3.

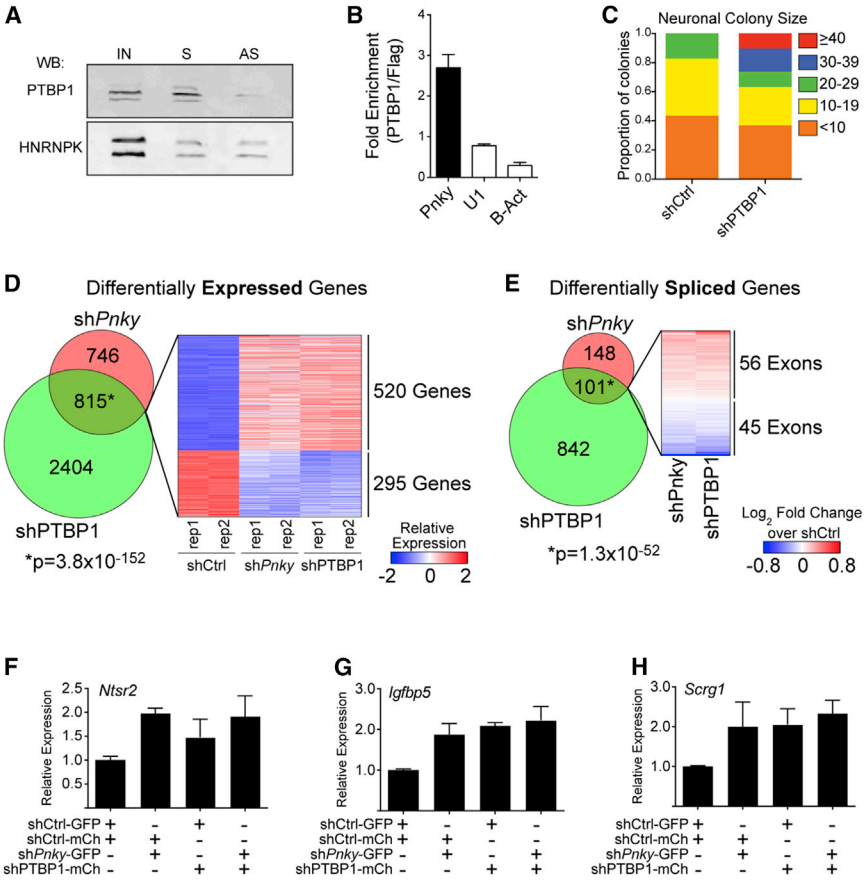

Figure 4. *Pinky* Interacts with PTBP1 and Regulates Transcript Expression and Differential Splicing

(A) Immunoblot for PTBP1 or HNRNPK after RNA pulldown with biotin-labeled sense (S) or antisense (AS) *Pnky* RNA incubated with V-SVZ NSC nuclear extract. IN, input V-SVZ nuclear extract.

(B) RT-qPCR detection for indicated RNA recovered by PTBP1-specific antibody normalized to control FLAG antibody. Error bars are propagated SD from technical triplicates.

(C) Quantification of number of TUJ1+ NBs found in individual neurogenic colonies with PTBP1-KD or control.

(D) Venn Diagram demonstrating the overlap between genes differentially expressed (FDR < 0.05) upon PTBP1-KD or *Pnky*-KD. Heatmap representation of the differential expression of the overlapping gene set in shCtrl, sh*Pnky*, and sh*Ptbp1* biological duplicate cultures is shown.

(E) Venn Diagram demonstrating the overlap between exons showing differential usage (FDR < 0.01) upon PTBP1-KD or *Pnky*-KD. Heatmap representation of the differential usage of the overlapping gene set in sh*Pnky* and sh*Ptbp1* cultures compared to control is shown.

(F–H) RT-qPCR detection of expression of indicated genes normalized to *Gapdh*. Expression in each condition is shown relative to control (shCtrl-GFP, shCtrl-mCherry). Error bars are 95% confidence intervals from three separate cultures. See also Figure S4 and Table S1, Table S2, and Table S3.

nonspecifically bound other RNA binding proteins including HNRNPK and ELAVL1 (Figures 4A and S4C), only *Pnky* RNA enriched for PTBP1, suggesting that the interaction between *Pnky* and PTBP1 is specific (Figure 4A). Furthermore, RNA immunoprecipitation with PTBP1 antibodies enriched for *Pnky* transcript, but not U1 or beta-actin mRNA (Figure 4B).

PTBP1 is expressed in NSCs and functions as a repressor of neuronal differentiation. In the embryonic brain, loss of *Ptbp1* results in precocious neuronal differentiation (Shibasaki et al., 2013), and in fibroblasts, *Ptbp1* knockdown leads to direct neuronal trans-differentiation (Xue et al., 2013). PTBP1 was detected in the nucleus of V-SVZ NSCs (Figure S4D), and PTBP1 knockdown resulted in larger neuronal colonies (Figure 4C), similar to the phenotype observed with *Pnky*-KD (Figure 2D).

In NSCs, PTBP1 negatively regulates the expression of *Ptbp2*, which is required for the generation of neuronal precursors (Boutz et al., 2007; Licatalosi et al., 2012). Using a PTBP2-specific antibody (Polydorides et al., 2000), we found that the *Pnky* transcript did not specifically bind PTBP2 (Figure S4E). During neurogenesis, *Ptbp1* is normally downregulated, and *Ptbp2* is increased (Keppetipola et al., 2012). Therefore we next characterized the relationship between *Ptbp1*, *Ptbp2*, and *Pnky* expression. Upon PTBP1 knockdown in V-SVZ NSCs, *Ptbp2* transcripts were upregulated, as expected (Figure S4F). PTBP1 knockdown did not decrease *Pnky* expression (Figure S4F). *Pnky*-KD had no effect on *Ptbp1* expression and caused a small reduction (25%) in *Ptbp2* (Figure S4G). Thus, the increase in neuronal differentiation observed with *Pnky*-KD does not appear to relate to changes in *Ptbp1* or *Ptbp2* expression.

PTBP1 regulates mRNA transcript levels and pre-mRNA splicing during neuronal differentiation (Keppetipola et al., 2012; Yap et al., 2012; Zheng et al., 2012). To determine whether *Pnky* and PTBP1 regulate a common set of transcripts, we performed RNA-seq of V-SVZ NSCs with either *Pnky*-KD or PTBP1-KD. The overlap of differentially expressed genes was highly significant (Figure 4D and Table S1, 815 genes, $p = 3.8 \times 10^{-152}$) and enriched for Gene Ontology terms (Huang et al., 2009) related to cell-cell adhesion, synaptogenesis, and neurogenesis (Table S2). Furthermore, using DEXSeq (Anders et al., 2012) to analyze differential exon usage, we found that *Pnky*-KD and PTBP1-KD also resulted in a common set of splice variants (Figure 4E and Table S3 101 exons, $p = 1.3 \times 10^{-52}$). Thus, these data demonstrate that *Pnky* and its associated protein PTBP1 regulate an overlapping set of transcripts that underlies their role in regulating neurogenesis from V-SVZ NSCs.

To further assess whether *Pnky* and PTBP1 function in the same pathway, we performed an epistasis experiment. The lack of synergistic or additive effects upon combined loss of an lncRNA and coding gene pair suggests that they function in the same molecular pathway (Dimitrova et al., 2014). Therefore, we used FACS to isolate NSCs with double knockdown of *Pnky* and PTBP1 as well as NSCs with each single knockdown (Figures S4H and S4I). We then analyzed the expression of several genes (*Ntsr2, Igfbp5*, *Scrg1*, and *Ppp1r3c*) that had

been commonly upregulated by both *Pnky*-KD and PTBP1-KD in RNA-seq experiments (Figure 4D). As expected, *Ntsr2*, *Igfbp5*, *Scrg1*, and *Ppp1r3c* all had increased expression in the cells with single knockdown as compared to control (Figures 4F–4H and S4J). Importantly, the combined knockdown of *Pnky* and PTBP1 did not further enhance this gene expression (Figures 4F–4H and S4J). These data indicate a genetic interaction between *Pnky* and *Ptbp1* and suggest that they function in the same pathway to regulate gene expression in NSCs.

DISCUSSION

Taken together, our data indicate that *Pnky* is a conserved, neural-specific, nuclear lncRNA that interacts with PTBP1 and regulates the production of neurons from NSCs. While other lncRNAs have been found to function in CNS development—with lncRNA loss-of-function resulting in decreased neurogenesis (Bond et al., 2009; Chalei et al., 2014; Lin et al., 2014; Ng et al., 2013; Rapicavoli et al., 2011; Sauvageau et al., 2013; Ulitsky et al., 2011)—*Pnky*-KD increased the production of neurons, suggesting a distinct developmental role for this lncRNA in controlling neurogenesis from NSCs. Our data are consistent with a model in which *Pnky* serves to "restrain" neuronal commitment, regulating the production of young neurons from NSCs in the developing embryonic cortex as well as those in the postnatal V-SVZ.

In the developing cortex, we found that *Pnky*-KD resulted in an increase in young neurons and decreased the NSC population in the VZ. This did not appear to involve a change in the proliferation of the TA cells of this embryonic lineage. In V-SVZ NSCs from the postnatal brain, *Pnky*-KD also promoted neuronal differentiation, and we additionally observed greater numbers of divisions of the neurogenic progenitor cells. Thus, the phenotypes of *Pnky*-KD in these two very different NSC populations are largely similar in that neuronal differentiation is increased. Interestingly, *Pnky* does not appear to regulate all NSC populations, as we did not detect *Pnky* transcripts in the dentate gyrus, which harbors another population of adult NSCs.

Our studies indicated that *Pnky* interacts with PTBP1, which is a key regulator of neural development (Shibasaki et al., 2013). PTBP1 is also a powerful mediator of cell reprogramming (Xue et al., 2013), and its depletion from fibroblasts can lead to direct trans-differentiation into neurons. Moreover, PTBP1 is a potent driver of brain tumor growth and invasiveness (Ferrarese et al., 2014). During neuronal differentiation, PTBP1 is normally downregulated, and there is an increase in PTBP2. We did not find evidence for a specific interaction between *Pnky* and PTBP2 or other nuclear RNA-binding proteins such as HNRNPK and ELAVL1. These data suggest that *Pnky* and PTBP1—a splicing factor with critical functions in both normal development and brain tumors—are part of a specific ribonucleoprotein complex in NSCs.

Given this physical interaction between *Pnky* and PTBP1, we worked toward understanding whether this lncRNA and protein partner function together. First, we found that both *Pnky* and PTBP1 knockdown in V-SVZ NSCs promoted neurogenesis. Furthermore, *Pnky*-KD promoted neuronal differentiation in the developing cortex, and mice with *Ptbp1* loss-of-function also exhibit precocious cortical neurogenesis. Thus, *Pnky*-KD and loss of PTBP1 produce similar phenotypic results. Second, we found that *Pnky*-KD and PTBP1-KD produced gene expression changes as well as splicing changes that were highly similar, indicating that *Pnky* and PTBP1 regulate a common set of transcripts related to neuronal differentiation. Third, our epistasis experiment indicated that *Pnky* and PTBP1 double knockdown does not produce changes greater than single knockdowns. Thus, the physical interaction between *Pnky* and PTBP1 along with the evidence for their genetic interaction is consistent with a model in which they function together in a common molecular pathway. Whether the physical interaction between *Pnky* and PTBP1 is required for their regulation of neuronal differentiation remains to be tested directly. Future work may reveal an interplay between lncRNAs and PTBP1 in different biological contexts, including cancer and direct cell reprogramming.

EXPERIMENTAL PROCEDURES

V-SVZ NSC Cultures

Postnatal day 5–7 (P5–7) C57BL/6 mouse brains were used to derive V-SVZ cultures, and cells were split 1:2 to passage 5 or 6 before they were switched from self-renewal to differentiation medium as described (Park et al., 2014).

ISH

Branched DNA ISH was performed in vitro and on adult tissue with the RNAScope 2.0 high definition BROWN kit (ACD). ISH on embryonic tissue was performed as described (Wallace and Raff, 1999) with DIG-labeled RNA probes.

Time-Lapse Imaging

Cultures were established by trypsinization and subsequent mixing of infected cultures (shCtrl or sh*Pnky*) with wild-type cells at a ratio of 1:200 to give ~15 GFP+ cells per high power field. Cultures were switched to differentiation medium and imaged on a Leica SP5 inverted confocal microscope fitted with a Life Imaging Services microscope temperature control system. Eight optical sections were taken every 15 min for 3 days. Cell fate was determined by morphology, and representative fields were analyzed by ICC for TUJ1 and GFAP.

Human Fetal Tissue

Fetal cortical tissue was collected from elective pregnancy termination specimens at San Francisco General Hospital, usually within 2 hr of the procedure. Research protocols were approved by the UCSF Committee on Human Research.

In Utero Electroporation

In utero electroporation was performed on E13.5 embryos from timed-pregnant wild-type Swiss-Webster mice (Simonsen labs) as described (Saito, 2006). Constructs used were pSicoR-shLuciferase (shCtrl) and pSicoR-sh*Pnky*-2 (sh*Pnky*). Embryos were harvested 48 hr later. One to three non-adjacent coronal sections per brain were imaged for quantification. Four animals from three separate surgeries were quantified for each experiment.

RNA Pulldown and Mass Spectrometry

Biotinylated RNA pulldown was performed as in Hacisuleyman et al. (2014). Selected SDS-PAGE-separated bands were excised and in-gel digested with trypsin as in Jiménez et al. (2001). LC-MS analyses of tryptic peptides utilized LTQ Orbitrap Velos mass spectrometer (Thermo Scientific) equipped with a NanoLC Ultra System (Eksigent) as described in Roan et al. (2014).

RNA-seq Analysis

Cluster generation and high-throughput sequencing were performed on a HiSeq 2500 (Illumina) using the paired-end 100 bp protocol. Reads were

aligned to the mouse genome mm9 using Tophat v2.0.10 (Trapnell et al., 2009). Differential expression was assessed using Cuffdiff v2.1.1 (Trapnell et al., 2010). Alternative splicing was analyzed using DEXSeq v1.8.0 (Anders et al., 2012), using an FDR threshold of 0.01.

ACCESSION NUMBERS

The NCBI GEO accession number for the RNA-seq data reported in this paper is GSE65542. The GenBank accession number for the mouse *Pnky* sequence is KP881340. The GenBank accession number for the human *PNKY* sequence is KP881341.

SUPPLEMENTAL INFORMATION

Supplemental Information for this article includes four figures, Supplemental Experimental Procedures, and three tables and can be found with this article online at http://dx.doi.org/10.1016/j.stem.2015.02.007.

AUTHOR CONTRIBUTIONS

A.D.R. and R.E.A. designed and performed experiments, interpreted data, and wrote the manuscript. S.J.L. performed RNA-seq analysis. T.J.N. performed in utero electroporations and human tissue staining. C.C.G. assisted with time-lapse imaging. S.J.H. processed and interpreted electroporation experiments. R.D.S. developed biochemical assays. H.Z. performed histological work. D.A.L. supervised research and helped write the manuscript. All authors edited the manuscript.

ACKNOWLEDGMENTS

We thank Robert Darnell for the PTBP2 antibody; David Weinberg for helpful discussions; Kenneth Probst for help with the graphical abstract; and Ewa Witkowski, Steven Hall, and The Sandler-Moore Mass Spectrometry Core Facility at UCSF for help with mass spectrometry. This project was supported by NIH DP2-OD006505-01, VA 1I01 BX000252-04, and a Shurl and Kay Curci Foundation Award to D.A.L; NIH R01 NS35710 to A.R.K.; NIH 1F31NS080501-01A1 to A.D.R.; National Science Foundation Graduate Research Fellowship Grant No. 1144247 to R.E.A.; MSTP training grant 2T32GM007618-34 to S.J.L.; SFSU CIRM Bridges TB1-01194 fellowship to S.H.; HHMI Medical Research Fellowship to H.Z.; and facilities and resources provided by the San Francisco Veterans Affairs Medical Center.

Received: August 14, 2014
Revised: January 13, 2015
Accepted: February 10, 2015
Published: March 19, 2015

REFERENCES

Anders, S., Reyes, A., and Huber, W. (2012). Detecting differential usage of exons from RNA-seq data. Genome Res. *22*, 2008–2017.

Batista, P.J., and Chang, H.Y. (2013). Long noncoding RNAs: cellular address codes in development and disease. Cell *152*, 1298–1307.

Bond, A.M., Vangompel, M.J.W., Sametsky, E.A., Clark, M.F., Savage, J.C., Disterhoft, J.F., and Kohtz, J.D. (2009). Balanced gene regulation by an embryonic brain ncRNA is critical for adult hippocampal GABA circuitry. Nat. Neurosci. *12*, 1020–1027.

Boutz, P.L., Stoilov, P., Li, Q., Lin, C.-H., Chawla, G., Ostrow, K., Shiue, L., Ares, M., Jr., and Black, D.L. (2007). A post-transcriptional regulatory switch in polypyrimidine tract-binding proteins reprograms alternative splicing in developing neurons. Genes Dev. *21*, 1636–1652.

Chalei, V., Sansom, S.N., Kong, L., Lee, S., Montiel, J.F., Vance, K.W., and Ponting, C.P. (2014). The long non-coding RNA Dali is an epigenetic regulator of neural differentiation. eLife *3*, e04530.

Dimitrova, N., Zamudio, J.R., Jong, R.M., Soukup, D., Resnick, R., Sarma, K., Ward, A.J., Raj, A., Lee, J.T., Sharp, P.A., and Jacks, T. (2014). LincRNA-p21 activates p21 in cis to promote Polycomb target gene expression and to enforce the G1/S checkpoint. Mol. Cell *54*, 777–790.

Doetsch, F., Caillé, I., Lim, D.A., García-Verdugo, J.M., and Alvarez-Buylla, A. (1999). Subventricular zone astrocytes are neural stem cells in the adult mammalian brain. Cell *97*, 703–716.

Doetsch, F., Petreanu, L., Caille, I., Garcia-Verdugo, J.M., and Alvarez-Buylla, A. (2002). EGF converts transit-amplifying neurogenic precursors in the adult brain into multipotent stem cells. Neuron *36*, 1021–1034.

Ferrarese, R., Harsh, G.R., 4th, Yadav, A.K., Bug, E., Maticzka, D., Reichardt, W., Dombrowski, S.M., Miller, T.E., Masilamani, A.P., Dai, F., et al. (2014). Lineage-specific splicing of a brain-enriched alternative exon promotes glioblastoma progression. J. Clin. Invest. *124*, 2861–2876.

Hacisuleyman, E., Goff, L.A., Trapnell, C., Williams, A., Henao-Mejia, J., Sun, L., McClanahan, P., Hendrickson, D.G., Sauvageau, M., Kelley, D.R., et al. (2014). Topological organization of multichromosomal regions by the long intergenic noncoding RNA Firre. Nat. Struct. Mol. Biol. *21*, 198–206.

Huang, W., Sherman, B.T., and Lempicki, R.A. (2009). Systematic and integrative analysis of large gene lists using DAVID bioinformatics resources. Nat. Protoc. *4*, 44–57.

Ihrie, R.A., and Alvarez-Buylla, A. (2011). Lake-front property: a unique germinal niche by the lateral ventricles of the adult brain. Neuron *70*, 674–686.

Jiménez, C.R., Huang, L., Qiu, Y., and Burlingame, A.L. (2001). In-Gel Digestion of Proteins for MALDI-MS Fingerprint Mapping. (Hoboken, NJ, USA: John Wiley & Sons, Inc.).

Keppetipola, N., Sharma, S., Li, Q., and Black, D.L. (2012). Neuronal regulation of pre-mRNA splicing by polypyrimidine tract binding proteins, PTBP1 and PTBP2. Crit. Rev. Biochem. Mol. Biol. *47*, 360–378.

Kong, L., Zhang, Y., Ye, Z.-Q., Liu, X.-Q., Zhao, S.-Q., Wei, L., and Gao, G. (2007). CPC: assess the protein-coding potential of transcripts using sequence features and support vector machine. Nucleic Acids Res. *35*, W345–W349.

Kriegstein, A., and Alvarez-Buylla, A. (2009). The glial nature of embryonic and adult neural stem cells. Annu. Rev. Neurosci. *32*, 149–184.

Lee, J.T. (2012). Epigenetic regulation by long noncoding RNAs. Science *338*, 1435–1439.

Licatalosi, D.D., Yano, M., Fak, J.J., Mele, A., Grabinski, S.E., Zhang, C., and Darnell, R.B. (2012). Ptbp2 represses adult-specific splicing to regulate the generation of neuronal precursors in the embryonic brain. Genes Dev. *26*, 1626–1642.

Lin, M.F., Jungreis, I., and Kellis, M. (2011). PhyloCSF: a comparative genomics method to distinguish protein coding and non-coding regions. Bioinformatics *27*, i275–i282.

Lin, N., Chang, K.-Y., Li, Z., Gates, K., Rana, Z.A., Dang, J., Zhang, D., Han, T., Yang, C.-S., Cunningham, T.J., et al. (2014). An evolutionarily conserved long noncoding RNA TUNA controls pluripotency and neural lineage commitment. Mol. Cell *53*, 1005–1019.

Lois, C., and Alvarez-Buylla, A. (1994). Long-distance neuronal migration in the adult mammalian brain. Science *264*, 1145–1148.

Lui, J.H., Hansen, D.V., and Kriegstein, A.R. (2011). Development and evolution of the human neocortex. Cell *146*, 18–36.

Luskin, M.B. (1998). Neuroblasts of the postnatal mammalian forebrain: their phenotype and fate. J. Neurobiol. *36*, 221–233.

Mercer, T.R., and Mattick, J.S. (2013). Structure and function of long noncoding RNAs in epigenetic regulation. Nat. Struct. Mol. Biol. *20*, 300–307.

Ng, S.-Y., Bogu, G.K., Soh, B.S., and Stanton, L.W. (2013). The long noncoding RNA RMST interacts with SOX2 to regulate neurogenesis. Mol. Cell *51*, 349–359.

Park, D.H., Hong, S.J., Salinas, R.D., Liu, S.J., Sun, S.W., Sgualdino, J., Testa, G., Matzuk, M.M., Iwamori, N., and Lim, D.A. (2014). Activation of neuronal gene expression by the JMJD3 demethylase is required for postnatal and adult brain neurogenesis. Cell Rep. *8*, 1290–1299.

Pastrana, E., Cheng, L.-C., and Doetsch, F. (2009). Simultaneous prospective purification of adult subventricular zone neural stem cells and their progeny. Proc. Natl. Acad. Sci. USA *106*, 6387–6392.

Peretto, P., Merighi, A., Fasolo, A., and Bonfanti, L. (1997). Glial tubes in the rostral migratory stream of the adult rat. Brain Res. Bull. *42*, 9–21.

Polydorides, A.D., Okano, H.J., Yang, Y.Y., Stefani, G., and Darnell, R.B. (2000). A brain-enriched polypyrimidine tract-binding protein antagonizes the ability of Nova to regulate neuron-specific alternative splicing. Proc. Natl. Acad. Sci. USA *97*, 6350–6355.

Ponti, G., Obernier, K., and Alvarez-Buylla, A. (2013). Lineage progression from stem cells to new neurons in the adult brain ventricular-subventricular zone. Cell Cycle *12*, 1649–1650.

Ramos, A.D., Diaz, A., Nellore, A., Delgado, R.N., Park, K.-Y., Gonzales-Roybal, G., Oldham, M.C., Song, J.S., and Lim, D.A. (2013). Integration of genome-wide approaches identifies lncRNAs of adult neural stem cells and their progeny in vivo. Cell Stem Cell *12*, 616–628.

Rapicavoli, N.A., Poth, E.M., Zhu, H., and Blackshaw, S. (2011). The long noncoding RNA Six3OS acts in trans to regulate retinal development by modulating Six3 activity. Neural Dev. *6*, 32.

Rinn, J.L., and Chang, H.Y. (2012). Genome regulation by long noncoding RNAs. Annu. Rev. Biochem. *81*, 145–166.

Roan, N.R., Chu, S., Liu, H., Neidleman, J., Witkowska, H.E., and Greene, W.C. (2014). Interaction of fibronectin with semen amyloids synergistically enhances HIV infection. J. Infect. Dis. *210*, 1062–1066.

Saito, T. (2006). In vivo electroporation in the embryonic mouse central nervous system. Nat. Protoc. *1*, 1552–1558.

Sauvageau, M., Goff, L.A., Lodato, S., Bonev, B., Groff, A.F., Gerhardinger, C., Sanchez-Gomez, D.B., Hacisuleyman, E., Li, E., Spence, M., et al. (2013). Multiple knockout mouse models reveal lincRNAs are required for life and brain development. eLife *2*, e01749.

Shibasaki, T., Tokunaga, A., Sakamoto, R., Sagara, H., Noguchi, S., Sasaoka, T., and Yoshida, N. (2013). PTB deficiency causes the loss of adherens junctions in the dorsal telencephalon and leads to lethal hydrocephalus. Cereb. Cortex *23*, 1824–1835.

Trapnell, C., Pachter, L., and Salzberg, S.L. (2009). TopHat: discovering splice junctions with RNA-Seq. Bioinformatics *25*, 1105–1111.

Trapnell, C., Williams, B.A., Pertea, G., Mortazavi, A., Kwan, G., van Baren, M.J., Salzberg, S.L., Wold, B.J., and Pachter, L. (2010). Transcript assembly and quantification by RNA-Seq reveals unannotated transcripts and isoform switching during cell differentiation. Nat. Biotechnol. *28*, 511–515.

Ulitsky, I., Shkumatava, A., Jan, C.H., Sive, H., and Bartel, D.P. (2011). Conserved function of lincRNAs in vertebrate embryonic development despite rapid sequence evolution. Cell *147*, 1537–1550.

Wallace, V.A., and Raff, M.C. (1999). A role for Sonic hedgehog in axon-to-astrocyte signalling in the rodent optic nerve. Development *126*, 2901–2909.

Wang, L., Park, H.J., Dasari, S., Wang, S., Kocher, J.-P., and Li, W. (2013). CPAT: Coding-Potential Assessment Tool using an alignment-free logistic regression model. Nucleic Acids Res. *41*, e74–e74.

Xue, Y., Ouyang, K., Huang, J., Zhou, Y., Ouyang, H., Li, H., Wang, G., Wu, Q., Wei, C., Bi, Y., et al. (2013). Direct conversion of fibroblasts to neurons by reprogramming PTB-regulated microRNA circuits. Cell *152*, 82–96.

Yap, K., Lim, Z.Q., Khandelia, P., Friedman, B., and Makeyev, E.V. (2012). Coordinated regulation of neuronal mRNA steady-state levels through developmentally controlled intron retention. Genes Dev. *26*, 1209–1223.

Zheng, S., Gray, E.E., Chawla, G., Porse, B.T., O'Dell, T.J., and Black, D.L. (2012). PSD-95 is post-transcriptionally repressed during early neural development by PTBP1 and PTBP2. Nat. Neurosci. *15*, 381–388.